Turbulence Structure and Prediction of Interfacial Heat and Mass Transfer in Wavy-Stratified Flow

C. Lorencez, M. Nasr-Esfahany, and M. Kawaji
Dept. of Chemical Engineering and Applied Chemistry, University of Toronto, Toronto, Ont., Canada M5S 3E5

The turbulence structure of the liquid phase near a wavy gas-liquid interface in stratified flow was experimentally investigated in a 50 mm (H) × 100 mm (W) rectangular duct. The characteristic parameters of the organized motion under the liquid waves such as the frequency of appearance and length scale were estimated by using the variable-interval time-averaging and the photochromic dye activation techniques. These characteristics were used in a hybrid surface renewal-eddy cell model to predict the interfacial heat- and mass-transfer coefficients in stratified two-phase flow. The predictions for cocurrent and countercurrent flows agreed reasonably well with experimental data available in the literature.

Introduction

Interfacial transport of mass and heat in gas-liquid systems is encountered in many industries and involved in a wide variety of equipment and processes such as heat exchangers, boilers, steam condensers, cooling towers, gas absorbers, and chemical reactors. It is also receiving greater attention in recent years as global warming is thought to be related to CO_2 buildup in the atmosphere, and the rate of CO_2 absorption in large bodies of water is controlled by the interfacial transport mechanism.

In view of its importance, numerous experimental studies of interfacial mass and heat transport at moving gas-liquid boundaries such as on surfaces of liquid layers in contact with a gas have been performed in the past. Many investigators have also attempted to advance models and theories that can predict transport rates at gas-liquid interfaces, however, the lack of a complete understanding of the interfacial phenomena has made it difficult to accurately predict the transport rates and optimize the transfer processes.

In experimental mass-transfer research, gas absorption studies have been performed under different flow conditions, for example, in still liquids (Higbie, 1935), in turbulent open-channel flows with interfacial shear (Aisa et al., 1981; Jensen and Yuen, 1982; McCready and Hanratty, 1985) and without (Fortescue and Pearson, 1967; Komori et al., 1990) in wind-wave tanks (Mattingly, 1977; Broecker et al., 1978; Komori et al., 1993), and in rivers and oceans (Liss, 1973; Liss and Merlivat, 1986; Watson et al., 1991). Regarding theoretical developments, quasi-laminar diffusion theories which postulate the existence of flow structures near the interface were among the earliest attempts to predict the mass-transfer coefficients. Some suggested structures were stagnant thin films at the interface (Lewis and Whiteman, 1924), renewal of the surface with fresh unsaturated liquid (Higbie, 1935; Danckwerts, 1951; Rashidi et al., 1991), counterrotating eddy cells near the surface (Fortescue and Pearson, 1967), and a combination of the above, such as a hybrid surface renewal-eddy cell model (Komori et al., 1993). Other important attempts in the theoretical development include the eddy diffusivity theories, in which a model for the eddy diffusivity is formulated and used in the numerical simulation of the entire flow field (Levich, 1962; Davies, 1972; Ueda et al., 1977; Daly and Harlow, 1980).

In interfacial heat-transfer studies, experimental work has been reported for rapid condensation of vapor on a subcooled liquid layer for stratified flow, both cocurrent (Bankoff, 1980; Jensen and Yuen, 1982; Lim et al., 1984; Murata et al., 1992) and countercurrent (Kim and Bankoff, 1983; Kim et al., 1985). The resulting local heat-transfer coefficients for condensation have been generally expressed in the form of empirical power law correlations of the type, $Nu = aRe_G^b Re_L^c Pr^d$, where a, b, c, and d are empirical constants. Attempts to correlate the interfacial heat-transfer coefficient data in terms of turbulence properties have also been made based on an analogy between heat and mass transfer. These turbulence centered models follow modified correlations such as $Nu_t = aRe_t^b Pr^c$, where Nu_t and Re_t are the turbulent Nus-

Correspondence concerning this article should be addressed to M. Kawaji.

selt and Reynolds numbers defined by $Nu_t = h\lambda_t/k$ and $Re_t = u_t\ \lambda_t/\nu$, respectively. ($\lambda_t$ is characteristic length scale (m), and ν is kinematic viscosity (m^2/s).)

In spite of the extensive studies described above, the turbulent structures in the gas and liquid streams near the interface region of open-channel and stratified two-phase flows have only recently been visualized, and their characteristic parameters used in surface-renewal type models to predict the mass- and heat-transfer coefficients. Komori et al. (1990) and Rashidi et al. (1991) proposed such models to predict the coefficients for mass transfer across unsheared and sheared (cocurrent and countercurrent), but smooth interfaces in turbulent open channel flows, respectively. For the case of a wavy gas-liquid interface in a wind-wave tank, Komori et al. (1993) used a hybrid surface renewal-eddy cell model to estimate the mass-transfer coefficients. A significant development in their model is the hypothesis that the surface renewal does not occur continuously. Murata et al. (1992) also used a surface-renewal type model to predict local heat-transfer coefficients in direct contact condensation experiments in stratified, two-phase flow with smooth and wavy gas-liquid interfaces. Reasonable agreement between Murata et al.'s predictions and experimental data was obtained although the frequency of the organized motion used in the model was estimated from an existing theory.

Thus, the main objective of this study was to experimentally investigate the relationship between the interfacial shear and the characteristics of the organized motion under the wavy gas-liquid interface in cocurrent and countercurrent, wavy-stratified two-phase flows. In addition, the parameters characterizing the organized motion were used in a hybrid surface renewal-eddy cell model to successfully predict the mass- and heat-transfer coefficient data in the literature.

Experiments

The experiments were conducted using a two-phase flow loop which included a rectangular flow channel and auxiliary components for investigating cocurrent and countercurrent stratified flows, as shown in Figure 1. The test channel was formed by three 2.40 m long sections of a rectangular channel, 100 mm wide and 50 mm high, which were joined end-to-end by flanges and assembled to ensure that the inside channel walls were flush. The working fluids were air and kerosene (Van-Sol 715), and the experiments were conducted at near atmospheric pressure and room temperature. A measurement station, including an optical window for the Photochromic Dye Activation technique and a hot-film anemometer port, was located in the ceiling of the test channel at a distance L = 440 cm from the liquid inlet, which was considered to be sufficient to ensure fully developed flow.

Photochromic dye activation technique

A nonintrusive photochromic tracer technique was used to visualize the instantaneous motion of the liquid near the interface. A photochromic dye 1',3',3'-trimethylindoline-6-nitrobenzospiropyran (TNSB), with an ultraviolet (UV) absorption spectrum and soluble only in organic liquids was dissolved in dilute concentration in kerosene, a clear liquid. Since its initial development (Popovich and Hummel, 1967), the photochromic dye activation technique has been used to investigate a variety of single-phase flow problems (Iribarne et al., 1972; Seeley et al., 1975, among many others). In these earlier studies, only a limited amount of quantitative measurements could be obtained due to various problems. Recent improvements (Kawaji et al., 1993; Lorencez, 1994; Lorencez et al., 1993) have significantly reduced these shortcomings. Modifications of the optics have resulted in sharper and thinner traces, which have improved the overall accuracy of the velocity measurements, especially near the moving gas-liquid interfaces.

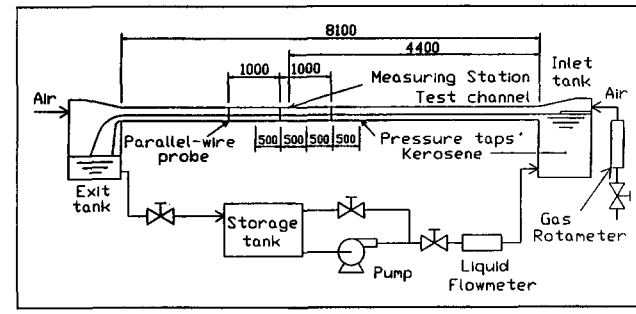

Figure 1. Experimental apparatus.

In the present work, pulsed UV light with a wavelength of 351 nm from an EXCIMER laser (Series TE-860-4 from Lumonics) was focused using two lens arrays with a focal length of 250 mm. Each lens array produced five traces in the photochromic solution, and the two main beams were intersected to form a 5×5 photochromic grid as shown in Figure 2. The traces are formed as the photochromic dye molecules in the path of the laser beam are activated and a dark color appears in the liquid containing the activated dye molecules. The concentration of the dye in the liquid can be adjusted to optimize the penetration depth of the UV light beam and the contrast of the traces formed. The present results were obtained with a dye concentration of approximately 0.01% by weight. The optical system was adjusted to create narrow, sharp intersecting traces in the liquid. Care was taken to ensure that the traces were formed at the central vertical plane to be viewed from the side of the test section.

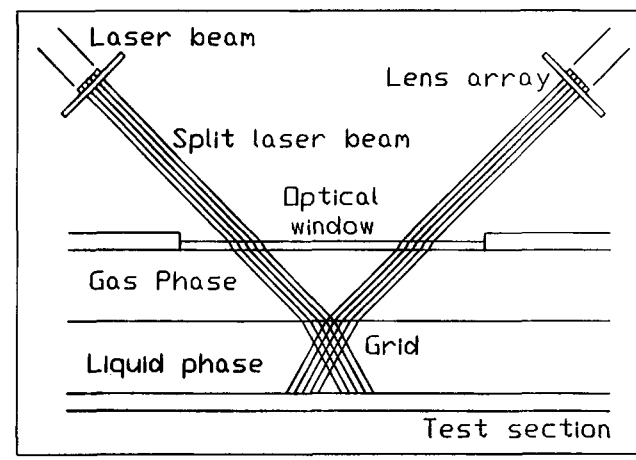

Figure 2. Grid formation using PDA technique.

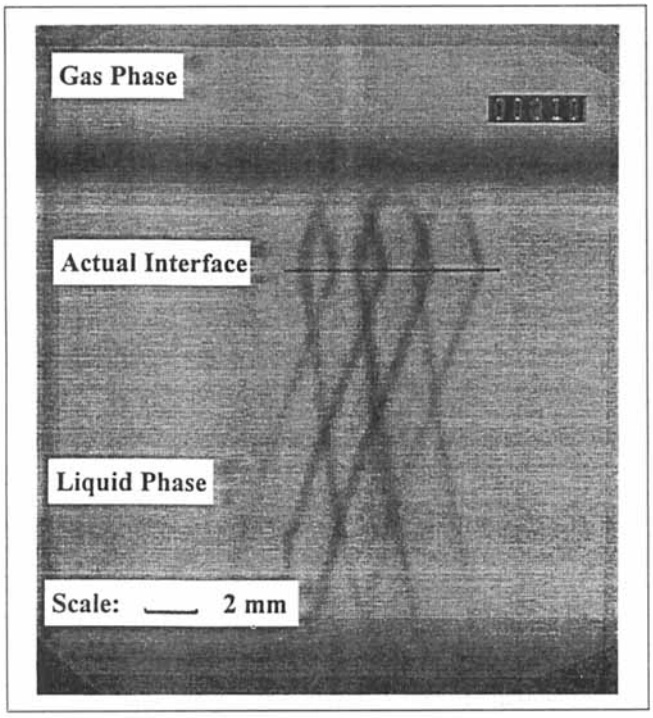

Figure 3. Grid pattern formed with PDA technique.

The motion of the traces in the liquid phase was recorded with a PHOTRON High Speed Video Camera, which was positioned horizontally facing the side of the channel and inclined slightly upward (8 deg) to view the traces from slightly below the interface. This way, obstruction of the view by the surface waves which occurred when viewed parallel to the interface was avoided. This arrangement allowed accurate determination of the interface position and shape at the plane of the trace formation since the liquid surface acted as a mirror and reflected the trace images as shown in Figure 3. The digital data stored in the high speed video camera system were later transferred to and analyzed in a microcomputer-based image analysis system.

Hot-wire anemometry

In addition to the photochromic dye activation method described above, a hot-film anemometer (Dantec 5601 and 56C17 bridges) with a cross wire film probe (Dantec 55R63) was used to measure the velocity profiles in the liquid and gas phases. Two differential input channels were simultaneously sampled at a rate of 1 kHz/channel for 60 s. In addition, a single wire probe (Dantec 55R14) was used to collect the data, which were used to detect the presence of organized motions, as described in a later section. Calibration of the hot-film probe in kerosene at low velocities was performed using a method similar to that proposed by Hirano et al. (1989). Data sampling was performed using a digital data acquisition system installed in a microcomputer.

The VITA (variable-interval time-averaging) technique was applied to estimate the frequency of appearance of the organized motions near the gas-liquid interface. This conditional averaging technique was developed by Blackwelder and Kaplan (1976) while studying the turbulence structure near the wall in a turbulent boundary layer, and has been previously used to estimate the frequency of appearance of the organized motions near the gas-liquid interface (Komori et al., 1989, 1993).

Briefly, the VITA technique is applied to a fluctuating quantity such as the streamwise velocity $U(t)$ (m/s). The variable-interval time average is then defined by

$$\hat{U}(t,T)=\frac{1}{T}\int_{t-1/2T}^{t+1/2T}U(s)ds, \tag{1}$$

where T is the averaging time (s). As T becomes larger, the conventional time averaging results, that is

$$\overline{U}=\lim_{T\to\infty}\hat{U}(t,T) \tag{2}$$

which is independent of t (time, s). To obtain a local average of a certain parameter of interest, the averaging time T must be of the same order of magnitude as the time scale of the phenomenon under study.

A localized measure of the turbulent energy is obtained by applying the VITA technique to the square of the streamwise velocity and subtracting the localized square mean value. This is called the localized variance and is defined by,

$$\text{var}(t,T)=U^2(t,T)-[\hat{U}(t,T)]^2, \tag{3}$$

which is a positive-definite quantity. The detection criterion is completed by using a threshold level k on the VITA variance signal. Thus, the detection function $D_v(t)$ is defined as

$$D_v=\begin{cases}1 & \text{if var}\,(t,T)>ku_{\text{rms}}^2,\\ 0 & \text{otherwise}\end{cases} \tag{4}$$

where u_{rms} is the conventional r.m.s. value of the total record of the velocity signal. The number of intervals in which $D_v(t)=1$ gives the number of appearances N_v of the organized motion. Then, the frequency of appearance is obtained from

$$f_L=N_V/T_{\text{sampling}} \tag{5}$$

In studying the bursting frequency in turbulent boundary layers, the recommended values for the dimensionless averaging time $T^+=Tu_{WL}^2/\nu$ and threshold level k are 10 and 1.0, respectively (Blackwelder and Kaplan, 1976; Chen and Blackwelder, 1978). (Subscript W is the wall, and subscript L is liquid phase). However, it has been found (Rashidi and Banerjee, 1990) that frequencies of the ejections and bursts scale with the local variables regardless of the nature of the boundary (no-slip or free-slip), and therefore, in this work, the dimensionless averaging time used was $T^+=Tu_{*L}^2/\nu=10$ with a threshold level $k=1.0$.

It should be noted that different values of f_L can be obtained by choosing other values of the threshold level, and therefore, the absolute value of f_L cannot be determined

Table 1. Experimental Conditions for Cocurrent Wavy-Stratified Flow

Run No.	$^*Q_L \times 10^4$ m^3/s	$Q_G \times 10^3$ m^3/s	$^*h_L$ mm	$^*\Delta h$ mm	f Hz	λ cm	Re_L	Re_G
100	4.56	8.10	15.3	0.4	11.0	5.5	7,760	7,990
101	4.56	8.89	15.2	0.6	12.7	5.4	7,770	8,770
102	4.56	9.72	14.5	0.9	9.1	6.4	7,840	9,540
103	4.56	10.52	14.0	1.9	8.8	7.7	7,920	10,280
104	4.56	11.20	13.5	2.2	8.3	7.5	7,980	10,900
105	4.56	12.02	12.0	2.8	9.1	7.9	8,170	11,580
110	3.51	8.10	13.0	0.3	9.0	6.7	6,200	7,860
111	3.51	8.89	13.0	0.6	11.6	5.5	6,200	8,610
112	3.51	9.72	12.5	0.9	9.3	6.3	6,240	9,390
113	3.51	10.52	12.0	1.1	8.0	8.1	6,290	10,140
114	3.51	11.20	11.5	1.7	8.5	6.9	6,350	10,680
115	3.51	11.90	11.0	2.0	8.7	6.7	6,400	11,480
116	3.51	12.72	10.5	2.3	7.8	8.3	6,450	12,120
120	2.65	8.84	10.5	0.6	10.3	5.0	4,860	8,470
121	2.65	9.72	10.3	0.8	9.3	5.8	4,880	9,250
122	2.65	10.58	10.2	1.1	9.2	6.2	4,890	10,000
123	2.65	11.20	10.0	1.1	8.1	6.8	4,910	10,630
124	2.65	12.02	9.5	1.6	7.6	7.3	4,950	11,370
125	2.65	12.73	9.5	2.1	7.8	6.7	4,950	12,040

$^*h_L$ is liquid level (mm); Q is volumetric flow rate (m^3/s); Δh is interfacial wave amplitude (mm).

precisely with this technique. However, if k is held constant for all the data, the relative variation of f_L, which cannot be attributed to the threshold value chosen (Blackwelder and Heritonidis, 1983), will indicate the effect of the flow conditions on the occurrence of the organized motion. Also, since a small threshold value will yield higher frequencies as evident from Eq. 4, Komori et al.'s (1993) use of $k = 0.16$ as opposed to a standard value of 1.0 is thought to give much higher frequencies than the value that would otherwise be obtained with $k = 1.0$.

Experimental Conditions

To study the flow structure near the moving gas-liquid interface, cocurrent and countercurrent flows with a wavy interface at different gas and liquid volumetric flow rates were examined. The experimental conditions are summarized in Tables 1 and 2, which include the liquid and gas volumetric flow rates, liquid height, wave amplitude, wavelength and wave frequency, and the liquid and gas Reynolds numbers. The volumetric flow rates were determined with flowmeters and rotameters calibrated prior to the experiments. The liquid height and wave amplitude were measured with vertical parallel wire probes placed in the mid-plane of the test section while the wavelength was obtained from the high speed video recordings. The wave amplitude represents the rms value of the variation of the liquid height, and the Reynolds number was computed in terms of the hydraulic diameter for each phase.

Tables 3 and 4 show the interfacial friction velocity for the gas, the frequency of appearance of the organized motion, and the averaging time used with the VITA technique for cocurrent and countercurrent flows, respectively. The interfacial friction velocity for the gas u_{*iG}, was determined from

Table 3. Results Obtained with the VITA Technique for Cocurrent Flow

Run No.	u_{*iG} m/s	f_L 1/s	T s
100	0.144±0.014	0.64±0.08	0.560±0.097
101	0.180±0.013	0.70±0.08	0.360±0.049
102	0.241±0.012	1.38±0.20	0.203±0.019
103	0.305±0.011	2.42±0.08	0.127±0.009
104	0.385±0.010	3.66±0.12	0.079±0.004
105	0.462±0.009	3.51±0.14	0.055±0.002
110	0.137±0.013	0.68±0.01	0.630±0.106
111	0.169±0.013	0.82±0.06	0.411±0.056
112	0.207±0.012	0.90±0.02	0.275±0.030
113	0.265±0.011	1.52±0.14	0.160±0.013
114	0.336±0.010	3.12±0.10	0.104±0.006
115	0.406±0.010	3.70±0.04	0.072±0.004
116	0.450±0.010	3.60±0.04	0.058±0.003
120	0.164±0.012	0.70±0.06	0.439±0.059
121	0.196±0.012	0.84±0.04	0.307±0.035
122	0.237±0.011	1.12±0.18	0.210±0.019
123	0.287±0.011	1.78±0.08	0.144±0.010
124	0.350±0.010	2.54±0.01	0.096±0.006
125	0.388±0.010	3.08±0.02	0.078±0.005

Table 2. Experimental Conditions for Countercurrent Wavy-Stratified Flow

Run No.	$Q_L \times 10^4$ m^3/s	$Q_G \times 10^3$ m^3/s	h_L mm	Δh mm	f Hz	λ cm	Re_L	Re_G
200	3.17	9.14	9.8	0.0	5.5	4.4	5,890	8,660
201	3.17	9.87	9.8	0.0	5.0	4.9	5,890	9,390
202	3.17	9.91	10.0	0.0	4.5	5.3	5,870	10,170
203	3.17	10.72	10.5	0.0	4.5	5.0	5,820	9,410
204	3.17	12.02	10.5	0.3	5.5	5.0	5,820	11,450
210	4.58	8.10	12.4	0.3	5.0	6.0	8,200	7,820
211	4.58	8.89	12.4	0.3	4.5	6.2	8,240	8,590
212	4.58	9.64	12.6	0.4	4.5	4.8	8,160	9,330
213	4.58	10.47	12.9	0.4	5.0	5.0	7,980	10,150
214	4.58	10.90	13.0	0.3	5.0	5.3	8,040	10,570
220	5.51	8.10	13.7	0.3	5.5	5.0	9,500	7,890
221	5.51	8.91	13.8	0.3	5.0	5.1	9,450	8,690
222	5.51	9.64	13.9	0.3	5.0	6.0	9,350	9,410
223	5.51	10.00	14.0	0.3	4.5	6.4	9,190	9,810
224	5.51	10.35	14.2	0.4	4.5	8.0	9,190	10,120

Table 4. Results Obtained with the VITA Technique for Countercurrent Flow

Run No.	u_{*iG} m/s	f_L 1/s	T s
200	0.218±0.010	1.32±0.03	0.249±0.021
201	0.266±0.010	1.65±0.08	0.167±0.012
202	0.312±0.010	2.06±0.02	0.121±0.007
203	0.365±0.008	2.44±0.15	0.088±0.004
204	0.412±0.010	2.70±0.09	0.069±0.003
210	0.251±0.008	2.04±0.06	0.189±0.012
211	0.281±0.009	2.53±0.07	0.150±0.009
212	0.318±0.009	3.00±0.19	0.117±0.007
213	0.369±0.009	3.72±0.06	0.087±0.004
214	0.409±0.009	3.85±0.11	0.071±0.003
220	0.255±0.009	2.11±0.10	0.181±0.012
221	0.303±0.009	2.90±0.05	0.128±0.007
222	0.358±0.009	3.79±0.03	0.092±0.004
223	0.377±0.009	3.87±0.11	0.083±0.004
224	0.402±0.009	3.49±0.06	0.073±0.003

the interfacial shear stress computed following the method suggested by Sadatomi et al. (1993). This method involves a momentum balance in the gas phase, in which the four most important contributions are considered: the pressure gradient, wall-gas and interfacial shear stresses, and interfacial level gradient. The pressure drop was measured directly with a Baratron differential pressure transducer, a very accurate and sensitive device with 0.05% or 0.013 Pa uncertainty at a full scale of 26.66 Pa. For the wall shear stress, the wall friction factor was measured with the Baratron transducer in single-phase gas flow experiments. The interfacial liquid level and its gradient were measured with three pairs of parallel wire probes. Once all the terms other than the interfacial shear term were evaluated from the experimental measurements, the gas momentum balance equation was solved for the interfacial shear stress. The mean relative error in the determination of u_{*iG} was estimated to be 8%.

Results and Discussion

Results obtained with the PDA technique

The Photochromic Dye Activation technique was used to visualize the organized motion under the wavy, sheared gas-liquid interface and to estimate the characteristic length scale of the organized motion. Photochromic grids were instantaneously formed in the liquid below the interface and their displacement and deformation recorded by the high speed video camera were analyzed to yield the instantaneous velocity profiles. Kinematic and turbulence data obtained using the PDA technique are reported elsewhere (Lorencez et al., 1997); thus, the present discussions will deal with the detection of the organized motion under the interfacial waves.

Typical photochromic grid patterns formed and observed on the windward side of the waves in cocurrent and countercurrent gas-liquid flows are shown in Figures 4 and 5, respectively. Analyses of the grid motion showed that the presence of interfacial waves causes a nonuniform distribution of the interfacial shear stress along the wavy surface, a phenomenon similar to that previously reported by Zilker and Hanratty (1979) for a two-dimensional wavy solid wall. It was also observed that for cocurrent flow, the upper layer of the liquid was accelerated on the windward side due to the high gas shear imposed on the liquid surface, which deformed the grid pattern immediately after its formation. In contrast, for countercurrent flow, the upper layer of the liquid was decelerated because of the gas flowing in the opposite direction.

During the analysis, the near-interface and bottom wall regions in the liquid were carefully observed in search of the organized motions. Turbulent bursts generated near the bottom wall and interface were present in both cocurrent and countercurrent flows with a wavy interface. In cocurrent flow, the interfacial shear imposed on the liquid layer on the windward side of the interfacial waves was strong enough to create turbulent bursts at the interface. Most of the bursts originated immediately upstream of the crest of the waves in the liquid phase. In countercurrent flow, the greater relative velocity between the gas and liquid also resulted in large-amplitude waves, and the interfacial shear acting on the windward side of the waves created turbulent bursts just downstream of the crest of the waves in the liquid phase. In general, in the present wavy-stratified two-phase flow experiments, both types of turbulent bursts, one from the wall and another from the interface, were observed to travel readily across the entire liquid layer and maintain their integrity for considerable distances. However, the turbulent bursts from the wall dissipated quickly after arriving at the interface due to enhanced mixing caused by the waves.

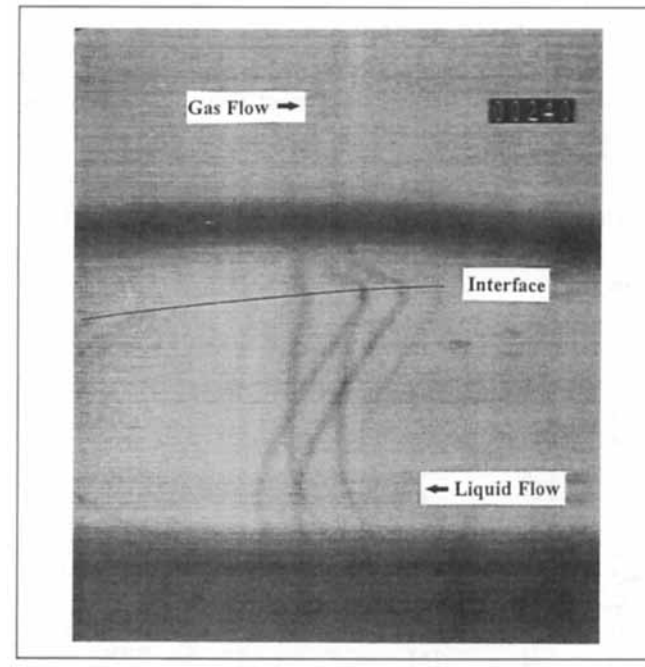

Figure 4. Photochromic traces formed on the windward side of a wave in cocurrent flow.

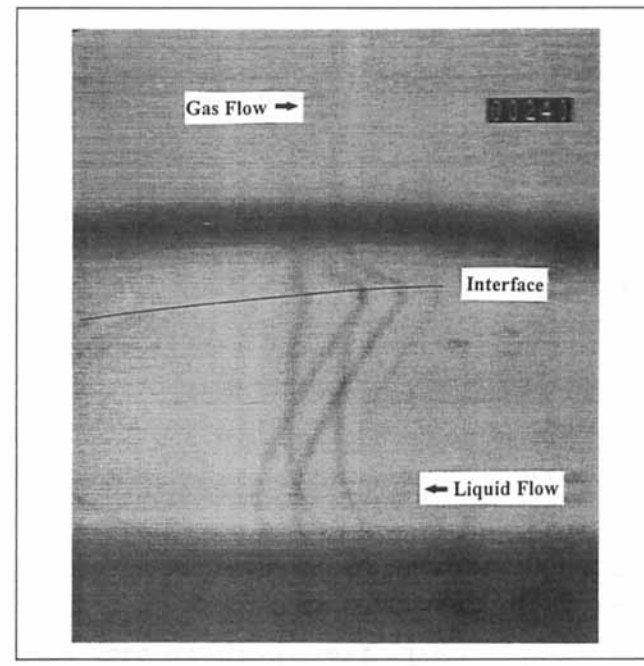

Figure 5. Photochromic traces formed on the windward side of a wave in countercurrent flow.

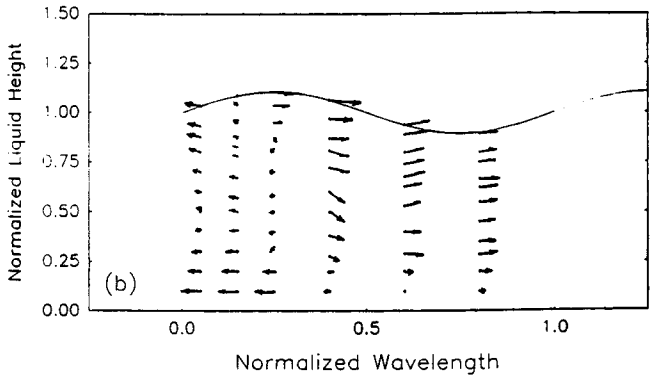

Figure 6. Mean velocity vectors under the wave as viewed from a frame of reference moving at the mean liquid velocity.

The vortex motion resulting from the turbulent bursts can be visualized from the motion of the photochromic grid when viewed in the frame of reference moving at the mean liquid velocity. The velocity vectors under different parts of the wave were first obtained by the ensemble averaging of the velocity data for many passing waves. The mean liquid velocity was then subtracted from the liquid velocity data to yield two-dimensional mapping of the velocity vectors in the liquid under the interfacial wave as shown in Figure 6. This figure shows a large vortex spanning nearly the entire liquid depth and about one-third of the wavelength in the axial direction. Therefore, it seemed appropriate to choose the height of the liquid layer as the characteristic length scale of the organized motion. In a parallel study to determine the vortex motion under the interfacial waves using a hot film probe, Nasr-Esfahany and Kawaji (1996) have obtained a plot of the flow field under the waves similar to that shown in Figure 6.

The video recordings were also analyzed to detect the existence of any organized motion of smaller scales such as minute eddies in periods between the interfacial turbulence bursts. However, no other types of organized motion except that induced by the interfacial turbulence bursts were observed under the wavy surface on either the windward or leeward side of the interfacial waves, or in the near wall region. Sketches illustrating the typical organized motion observed in cocurrent and countercurrent wavy flows described above are shown in Figure 7.

Due to the limitations of the experimental apparatus, it was not possible to quantify, with sufficient accuracy, the frequency of the appearance of the organized motions f_L (s^{-1}) based on flow visualization alone. However, it was possible to establish that f_L was similar in magnitude to the wave frequency. An accurate measurement of the frequency of turbulent bursts is described in the next section.

Results obtained with VITA technique

To study the interfacial turbulent bursts and the resulting vortex motion under the waves, a single wire hot-film probe was positioned slightly underneath the trough of the waves in order to generate an output signal containing a minimum of wall turbulent bursts information. As mentioned previously, the wall turbulent bursts quickly dissipated when they reached the upper layers of the liquid.

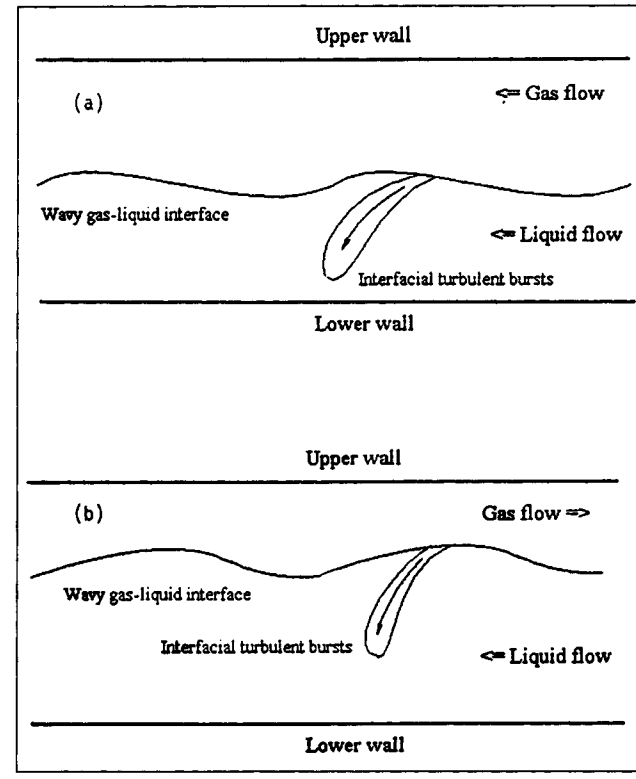

Figure 7. Sketches of turbulence bursts observed in (a) cocurrent flow and (b) countercurrent flow.

Similar ranges of values (between 0.5 and 0.05) were obtained for the averaging time T(s) in both cocurrent and countercurrent flows. Once the averaging time was known, the localized variance (Eq. 3) was calculated, and by using the detection function with a threshold level $k = 1.0$, the frequency of appearance f_L (Eq. 5) was obtained as shown in Tables 3 and 4. As noted previously, the values of f_L depend on the threshold level k used, but the frequencies shown can be used to study the dependence of f_L on flow parameters such as the interfacial friction velocity.

Figures 8 and 9 show the frequency of the organized motions in the liquid flow f_L (s^{-1})/s vs. the interfacial gas friction velocity u_{*iG} (m/s), for cocurrent and countercurrent flows, respectively. In both figures, the frequencies of appearance and the gas friction velocities have been normalized using the smallest value of each obtained in this study. In Figure 8, the frequencies increase rapidly with increasing u_{*iG} in the weakly sheared region ($u_{*iG} < 0.35$ m/s), but the rate of increase is reduced in the highly sheared region ($u_{*iG} >$ 0.35m/s). The relations between f_L and u_{*iG} in the weakly and highly sheared regions were different from the results of Rashidi and Banerjee (1990) for an open channel flow with a sheared but smooth interface, where the main mechanism of turbulence production is due to the interfacial turbulence bursts with a frequency of appearance proportional to u_{*iG}^2. In the present case, the turbulence is also generated by the interfacial waves, and therefore, the frequency of appearance of the organized motions is no longer solely proportional to u_{*iG}^2.

In countercurrent flow, although fewer experimental runs were conducted, the frequency of appearance increased with

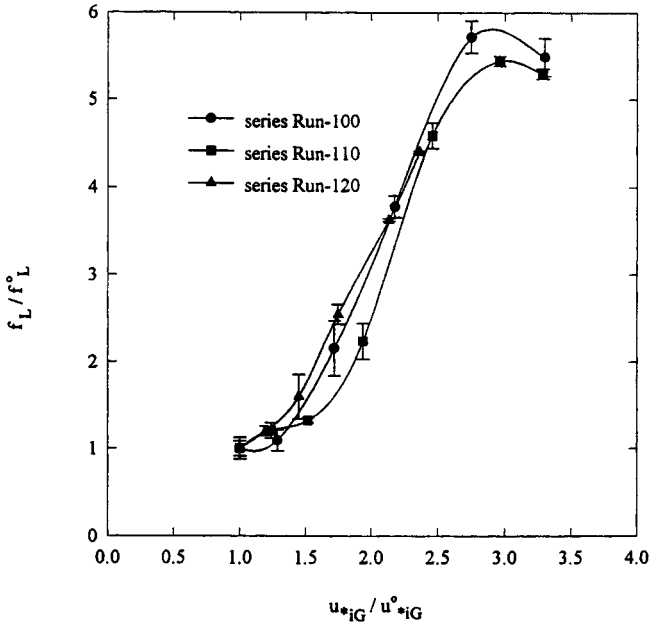

Figure 8. Variation of frequency of appearance of organized motions with the interfacial friction velocity in cocurrent flow.

increasing u_{*iG} in the weakly sheared region ($u_{*iG} < 0.35$m/s) in a manner similar to that observed for cocurrent flow. However, the frequency of appearance was not proportional to u_{*iG}^2 as shown in Figure 9, again due to the presence of large-amplitude interfacial waves. Because of the occurrence of the flow pattern transition to slug flow at higher gas flow rates, higher values of u_{*iG} could not be investigated for countercurrent flow.

It is worth noting that the present frequencies of the organized motions show significant differences from those reported by Komori et al. (1993) for the case of a wind-wave tank with a wavy interface. Using the VITA technique, they studied the organized motion under the interfacial waves in a 0.5 m deep liquid layer where the waves had a mean wavelength of 40-215 mm and a mean height of 1-12 mm. They reported averaging times and frequencies of appearance of the organized motion quite different from those measured in this work. Their averaging time T was given by a correlation such as

$$T = 0.003 u_{*iG}^{-0.92} \tag{6}$$

and a very low threshold level ($k = 0.16$) was used in the VITA technique. Consequently, they obtained frequencies of appearance in the range $10 < f_L < 80$ s^{-1}. As obvious from comparison with the present results, their averaging time is nearly one order of magnitude shorter and the frequency of appearance of the organized motions one order of magnitude greater than the corresponding results obtained in the present work. In addition the frequency of appearance of the organized motions obtained in Komori et al.'s work was much greater than the wave frequencies (ranging from 3.10-8.40 s^{-1}), while they were of comparable magnitudes or lower for cocurrent flow in our work. Then, it appears that the discrepancies between Komori et al.'s data and those reported in this work may be due to the difference in interpretation and use of the VITA technique.

Also, based on flow visualization work, Komori et al. (1993) postulated the existence of numerous minute surface-renewal eddies occurring along the windward side of the interfacial waves, in addition to the intermittent, large-scale downward turbulent bursts (see Figure 11 in their article). However, by using the PDA technique in this work, no such minutes eddies were found near the gas-liquid interface and only relatively large vortices spanning nearly the entire depth of the

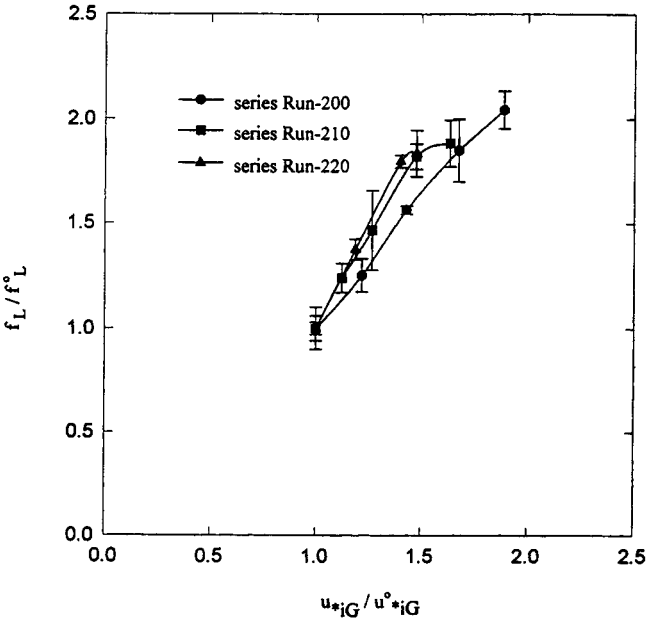

Figure 9. Variation of frequency of appearance of organized motions with the interfacial friction velocity in countercurrent flow.

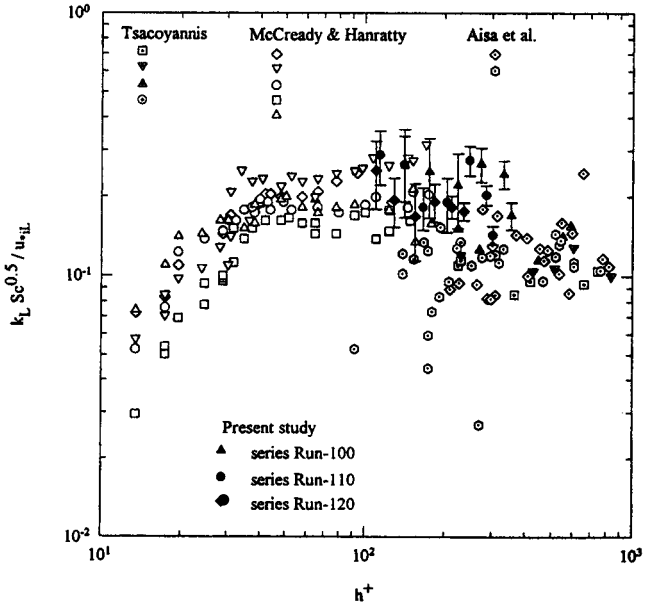

Figure 10. Comparison of predicted and measured gas absorption mass-transfer coefficients for cocurrent flow.

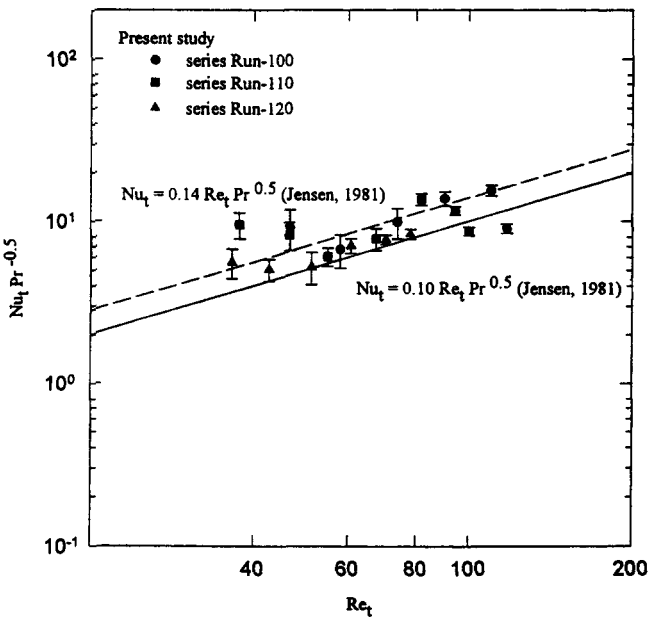

Figure 11. Comparison of predicted and experimental correlations for heat-transfer coefficients in cocurrent flow.

liquid layer and produced by downward interfacial turbulent bursts were observed under the waves. Apart from the obvious differences between the two experimental configurations, a possible explanation for the lack of the minute eddies could be related to the smaller amplitude and shorter wavelength of the interfacial waves and the lower interfacial friction velocity investigated in this study. An exact physical explanation for the differences observed in the characteristics of the organized motions under the interfacial waves in a thin liquid layer (< 20 mm) flowing in a rectangular channel and a deep liquid layer (≈ 0.5 m) in a wind-wave tank requires a further investigation.

Prediction of mass- and heat-transfer coefficients

Since the surface-renewal motion is far from the ideal motion assumed in Higbie's model, and in addition, it does not renew the free surface continuously as in the Fortescue and Pearson's model, Brumfield et al. (1975) proposed an additional function $F(\tau_e)$ in the evaluation of the mass-transfer coefficient k_L

$$k_L = 0.7F(\tau_e)(D_L u_t/\lambda_t)^{1/2} \tag{7}$$

where $F(\tau_e)$ includes the time fraction in which the surface renewal occurs. Similarly, Komori et al. (1993) proposed a hybrid surface renewal-eddy cell model to explain their CO_2-absorption experiments in a wind-wave tank. In their model, the mass-transfer coefficient k_L (m/s) is given by

$$k_L = 0.9t^*(D_L f_L)^{1/2} \tag{8}$$

where t^* ($= Tf_L$) is also the time fraction in which the surface renewal occurs. The main advantage of this model is that it can be used to predict mass-transfer coefficients for other free surface problems whenever the appropriate parameters for the eddy cells are known.

The hybrid surface renewal-eddy cell model given by Eq. 8 and the values of T and f_L obtained were used to predict the interfacial mass- and heat-transfer coefficient data reported by others for flow configurations quite similar to that used in the present work. Since only the relative values of f_L obtained by the VITA technique are of significance, the values of f_L shown in Tables 3 and 4 could be adjusted to predict the mass- and heat-transfer coefficients. Therefore, the values of f_L which gave the best predictions were those listed in Tables 3 and 4 multiplied by a factor of two. This makes the frequency of appearance and wave frequency comparable, which is consistent with the observations of the photochromic dye traces as mentioned previously.

The predictions of the hybrid model were compared to detailed experimental gas absorption data for cocurrent, stratified two-phase flows reported by McCready and Hanratty (1985) for thin liquid layers ($h < 10$mm), and Tsacoyannis (1976) and Aisa et al. (1981) for thicker layers ($10 < h < 30$ mm). This comparison of predicted and experimental mass-transfer coefficient for cocurrent flow is shown in Figure 10. The coefficients predicted by the model agreed reasonably well with the experimental values of McCready and Hanratty for their thicker films in the region $h^+ \approx 100$, as well as with Aisa et al's data in the range $100 < h^+ < 300$, but they slightly overpredicted those of Tsacoyannis' data [h^+ is the nondimensional liquid level ($= h_L U_{*iG}/\nu$)]. For the case of countercurrent flow, no gas absorption data in horizontal stratified flow could be readily found in the literature for comparison with the model predictions.

The prediction of the interfacial heat-transfer coefficients can be accomplished using the hybrid surface renewal-eddy cell model and a heat- and mass-transfer analogy (Bankoff, 1980)

$$h = 0.7F(\tau_e)\rho C_{PL}(\alpha f_L)^{1/2} \tag{9}$$

where $F(\tau_e)$ includes the time fraction in which the surface renewal occurs. In this work, due to the simplicity of incorporating the time fraction of the surface renewal through the parameter t^* instead of a function, it is proposed to evaluate the heat-transfer coefficients using

$$h = t^*\rho C_{PL}(\alpha f_L)^{1/2} \tag{10}$$

where C_{PL} is specific heat (J/kg K), h is heat-transfer coefficient (W/m^{2}k), ρ is the density of fluid (kg/m^3), and α is thermal diffusivity (m^2/s). Jensen (1981) and Kim and Bankoff (1983) carried out detailed condensation heat-transfer measurements in horizontal cocurrent and countercurrent steam-water flows, respectively, in test sections and at liquid Reynolds numbers similar to those employed in this study. Both of them used turbulence-centered models based on their experimental data to explain the interfacial heat-transfer coefficients. Here, Eq. 10 and the characteristic parameters of the organized motion measured in this work were used to predict the interfacial heat-transfer coefficients.

The present model predictions are compared with the measured interfacial heat-transfer coefficients reported by

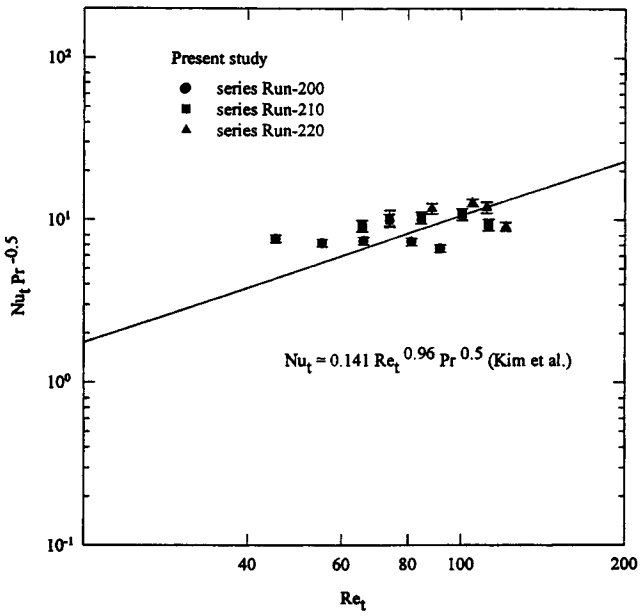

Figure 12. Comparison of predicted and experimental correlations for heat-transfer coefficients in countercurrent flow.

Jensen (1981) and Kim and Bankoff (1983) in Figures 11 and 12, for cocurrent and countercurrent flows, respectively. In the cocurrent flow case shown in Figure 11, the predicted values lie mostly in the region encompassed by Jensen's experimental correlations for high ($Nu_t = 0.14\ Re_t Pr^{0.5}$) and low ($Nu_t = 0.1\ Re_t\ Pr^{0.5}$) Reynolds numbers. ($Pr$ is the Prandtl number.) It is also noted that the model predictions (with some scatter) presented approximately a similar slope as the correlations. For countercurrent flow, the predicted heat-transfer coefficients agreed reasonably well with Kim and Bankoff's (1983) correlation, as shown in Figure 12 for the range of liquid Reynolds number tested in this work. The predictions for thick films slightly overpredicted the experimental correlation while those for thin films showed good agreement. The range of liquid Reynolds numbers covered in the present work is, however, limited and further work is required to verify the applicability of the present approach over a wider range of flow parameters.

Conclusions

The structure of turbulence existing under the wavy gas-liquid interface in cocurrent and countercurrent stratified flows in a rectangular channel has been investigated experimentally in connection with the interfacial transfer of mass, momentum, and energy. Both the photochromic dye activation method and hot film anemometry were used to investigate the characteristics of the organized motion occurring under the wavy interface.

Significant differences in the organized motion were observed between the wavy-stratified gas-liquid flow in a rectangular channel and a wavy flow in a wind-wave tank or in open channel flows. In the present work, a vortex spanning nearly the entire depth of the liquid layer was found to exist as a result of turbulence bursts occurring at the sheared, wavy interface. No minute eddies were found along the windward side of the interfacial waves as previously postulated for deep liquid layers in a wind-wave tank. The characteristic parameters of the organized motion under the wavy gas-liquid interface were shown to be applicable to the prediction of interfacial mass- and heat-transfer coefficients using a hybrid surface renewal-eddy cell model. Both the interfacial heat- and mass-transfer coefficients predicted using the model agreed reasonably well with the experimental data available in the literature for both cocurrent and countercurrent flows.

Acknowledgment

This work was supported by the Natural Sciences and Engineering Research Council of Canada and the Japan Atomic Energy Research Institute. A graduate scholarship awarded by Isfahan University of Technology to M. Nasr-Esfahany is gratefully acknowledged.

Literature Cited

Aisa, L., B. Caussade, J. George and L. Masbernat, "Echanges de Gaz Dissous en Ecoulements Stratifies de Gaz et de Liquide," *Int. J. Heat Mass Transf.* **24**(6), 1005 (1981).

Bankoff, S. G., "Some Condensation Studies Pertinent to LWR Safety," *Int. J. Multiphase Flow*, **6**, 51 (1980).

Blackwelder, R. F., and J. H. Haritonidis, "Scaling of the Bursting Frequency in Turbulent Boundary Layers," *J. Fluid Mech.*, **132**, 87 (1983).

Blackwelder, R. F., and R. E. Kaplan, "On the Wall Structure of the Turbulent Boundary Layer," *J. Fluid Mech.*, **76**, 89 (1976).

Broecker, H. C., K. Petermann, and W. Siems, "The Influence of Wind on CO_2-Exchange in Wind-Wave Tunnel, including the Effects of Monolayers," *J. Mar. Res.*, **36**, 595 (1978).

Brumfield, L. K., R. N. Houze, and T. G. Theofanous, "Turbulent Mass Transfer at Free, Gas-Liquid Interfaces, with Applications to Film Flows," *Int. J. Heat Mass Transf.* **18**, 1077 (1975).

Chen, C-H. P., and R. F. Blackwelder, "Large-Scale Motion in a Turbulent Boundary Layer: a Study Using Temperature Contamination," *J. Fluid Mech.*, **89**, 1 (1978).

Daly, B. J., and F. H. Harlow, "Numerical Study of Condensation in Cocurrent Stratified Flows," NUREG/CR-1108 (1980).

Danckwerts, P. V., "Significance of Liquid-Film Coefficients in Gas Absorption," *Ind. Eng. Chem.*, **43**, 1460 (1951).

Davies, J. T., *Turbulence Phenomena*, Academic Press, New York (1972).

Fortescue, G. E., and J. R. A. Pearson, "On Gas Absorption into a Turbulent Liquid," *Chem. Eng. Sci.*, **22**, 1163 (1967).

Higbie, R., "The Rate of Absorption of a Pure Gas Into a Still Liquid during Short Periods of Exposure," *Trans. AIChE.*, **31**, 365 (1935).

Hirano, S., S. Matsumoto, Y. Tanaka, and T. Yamamoto, "Calibration of Hot-Film Probes in Water at Low-Velocities," in *Dantec Information*, No. 8, 11 (1989).

Iribarne, I., F. Frantisak, R. L. Hummel, and J. W. Smith, "An Experimental Study of Instabilities and Other Flow Properties of a Laminar Pipe Jet," *AIChE J.*, **18**, 689 (1972).

Jensen, R. J., "Interphase Transport in Horizontal Stratified Cocurrent Flow," PhD Thesis, Dept. of Mechanical Engineering, Northwestern Univ., Evanston, IL (1981).

Jensen, R. J., and M. C. Yuen, "Interphase Transport in Horizontal Stratified Cocurrent Flow," NUREG/CR-2334 (1982).

Kawaji, M., W. Ahmad, J. deJesus, B. Sutharsan, C. Lorencez, and M. Ojha, "Flow Visualization of Two-Phase Flows Using Photochromic Dye Activation Method," *Nucl. Eng. and Des.*, **141**, 343 (1993).

Kim, H. J., and S. G. Bankoff, "Local Heat Transfer Coefficients for Condensation in Stratified Countercurrent Steam-Water Flows," *ASME Heat Transfer*, **105**, 706 (1983).

Kim, H. J., S. C. Lee and S. G. Bankoff, "Heat Transfer and Interfacial Drag in Countercurrent Steam-Water Stratified," *Int. J. Multiphase Flow*, **11**, (5), 593 (1985).

Komori, S., Y. Murakami, and H. Ueda, "The Relationship between Surface-Renewal and Bursting Motions in an Open-Channel Flow," *J. Fluid Mech.*, **203,** 103 (1989).

Komori, S., R. Nagaosa, and Y. Murakami, "Mass Transfer into a Turbulent Liquid Across the Zero-Shear Gas-Liquid Interface," *AIChE J.*, **36,** 957 (1990).

Komori, S., R. Nagaosa and Y. Murakami, "Turbulence Structure and Mass Transfer across a Sheared Air-Water Interface in Wind-Driven Turbulence," *J. Fluid Mech.*, **249,** 161 (1993).

Levich, V. G., *Physicochemical Hydrodynamics*, Prentice Hall, Englewood Cliffs, NJ (1962).

Lewis, W. K., and Whitman, W. G., "Principles of Gas Absorption," *Ind. Eng. Chem.*, **16,** 1215 (1924).

Lim, I. S., R. S. Tankin, and M. C. Yuen, "Condensation Measurements of Horizontal Cocurrent Steam/Water Flow," *ASME J. Heat Transf.*, **106,** 425 (1984).

Liss, P. S., "Process of Exchange Across an Air-Water Interface," *Deep-Sea Res.*, **20,** 221 (1973).

Liss, P. S., and L. Merlivat, "Air-Sea Gas Exchange Rates: Introduction and Synthesis," *The Role of Air-Sea Exchange in Geochemical Cycling*, P. Buat-Menard, ed. (1986).

Lorencez, C., "Turbulent Momentum Transfer at a Gas-Liquid Interface in a Horizontal Stratified Flow in a Rectangular Channel," PhD Thesis, Dept. of Chemical Engineering and Applied Chemistry, Univ. of Toronto, Toronto, Canada (1994).

Lorencez, C., M. Kawaji, M. Ojha, A. Ousaka, and Y. Murao, "Application of a Photochromic Dye Activation Method to Stratified Flow with Smooth and Wavy Gas-Liquid Interface," *ANS Proc. Heat Transfer Conf.*, Atlanta, HTC 7, 160 (1993).

Lorencez, C., M. Nasr-Esfahany, M. Kawaji, and M. Ojha, "Liquid Turbulence Structure at a Sheared and Wavy Gas-Liquid Interface," *Int. J. Multiphase Flow*, **23**(2), 205 (1997).

Mattingly, G. E., "Experimental Study of Wind Effects on Reaeration," *J. Hydraulics Div. ASCE*, HY3, **103,** 311 (1977).

McCready, M. J., and T. J. Hanratty, "Effect of Air Shear on Gas Absorption by a Liquid Film," *AIChE J.*, **31**(12), 2006 (1985).

Murata, A., E. Hihara, and T. Saito, "Prediction of Heat Transfer by Direct Contact Condensation at a Steam-Subcooled Water Interface," *Int. J. Heat Mass Transf.*, **35**(1), 101 (1992).

Nasr-Esfahany, M., and M. Kawaji, "Turbulence Structure Under a Typical Shear Induced Wave at a Liquid-Gas Interface," *AIChE Symp. Ser.*, **92** (310), 203 (1996).

Popovich, A. T., and R. L. Hummel, "A New Method for Non-Disturbing Turbulent Flow Measurements Very Close to a Wall," *Chem. Eng. Sci.*, **22,** 21 (1967).

Rashidi, M., and S. Banerjee, "The Effect of Boundary Conditions and Shear Rate on Streak Formation and Breakdown in Turbulent Channel Flows," *Phys. Fluids A.*, **2,** 1827 (1990).

Rashidi, M., G. Hetsroni, and S. Banerjee, "Mechanisms of Heat and Mass Transport at Gas-Liquid Interfaces," *Int. J. Heat Mass Transf.*, **34**(7), 1799 (1991).

Sadatomi, M., M. Kawaji, C. Lorencez, and T. Chang, "Prediction of Liquid Level Distribution in Horizontal Gas-Liquid Flows with Interfacial Level Gradient," *Int. J. Multiphase Flow*, **19**(6), 987 (1993).

Seeley, L. E., R. L. Hummel, and J. W. Smith, "Experimental Velocity Profiles in Laminar Flow Around Spheres at Intermediate Reynolds Numbers," *J. Fluid Mech.*, **68,** 591 (1975).

Tsacoyannis, Y., "Etude de l'Absorption d'un Gaz par un Liquide en Ecoulement Turbulent Stratifie," These de Docteur-Ingenieur, Universite Paul Sabatier de Toulouse (1976).

Ueda, H., R. Moller, S. Komori, and T. Mizushina, "Eddy Diffusivity near the Free Surface of Open Channel Flow," *Int. J. Heat Mass Transf.*, **20,** 1127 (1977).

Watson, A. J., R. C. Upstill-Goddard, and P. S. Liss, "Air-Sea Gas Exchange in Rough and Stormy Seas Measured by a Dual-Tracer Technique," *Nature*, **349,** 145 (1991).

Zilker, D. P., and T. J. Hanratty, "Influence of the Amplitude of a Solid Wave Wall on a Turbulent Flow. Part 2. Separated Flows," *J. Fluid Mech.*, **90,** 257 (1979).

Manuscript received Jan. 18, 1995, and revision received Sept. 25, 1996.